Implications of a Consensus Recognition Site for Phosphatidylcholine Separate from the Active Site in Cobra Venom Phospholipases A_2[†]

Angel R. Ortiz, M. Teresa Pisabarro, José Gallego, and Federico Gago*

Departamento de Fisiología y Farmacología, Universidad de Alcalá de Henares, 28871 Madrid, Spain

Received May 24, 1991; Revised Manuscript Received November 4, 1991

ABSTRACT: A model structure of *Naja naja kaouthia* cobra venom phospholipase A_2 has been constructed by utilizing molecular modeling techniques. Analysis of the model and available biochemical data reveal the presence in this enzyme of a putative recognition site for choline derivatives in loop 57–70 made up of residues Trp-61, Tyr-63, Phe-64, and Lys-65, together with Glu-55. The magnitude and shape of the electrostatic potential in this binding site are approximately 80% similar to that in the McPC603 antibody binding site specifically recognizing phosphocholine. Docking studies indicate that the recognition site we now describe and the phosphocholine head of an *n*-alkylphosphocholine molecule are complementary both sterically and electronically, mainly due to anion–cation and cation–π interactions. Moreover, binding enthalpies of *n*-heptylphosphocholine to this site are found to parallel the catalytic rate of pancreatic, mutant pancreatic, and cobra venom phospholipase A_2 enzymes acting on dihexanoylphosphatidylcholine micelles, suggesting that it behaves as an activator site. This proposal is in keeping with the "dual phospholipid" model put forward to account for the phenomenon of interfacial activation. This novel site is also shown to be able to discriminate choline derivatives from ethanolamine derivatives, in accord with experimental data. On the basis of the results obtained, two functions are assigned to this putative activator site: (i) desolvation of the lipid–enzyme interface, particularly the surroundings of tyrosine at position 69 (Tyr-63), and (ii) opening of the entrance to the active site by means of a conformational change of Tyr-63 whose χ_2 angle rotates nearly 60°.

The lipolytic enzyme phospholipase A_2 (PLA_2) splits the 2-acyl bond of L-1,2-diacylphosphatides in a calcium dependent, stereospecific, and stereoselective reaction (Dennis, 1983). Release of fatty acids, arachidonic acid in particular, provides the substrate required for the synthesis of eicosanoids, involved in pathophysiological processes such as inflammation, platelet aggregation, and acute hypersensitivity reactions (Mobilio & Marshall, 1989). Thus, modulation of PLA_2 activity is a current pharmacological goal, and there is a great interest in developing specific inhibitors for this enzyme in order to prevent, or suppress, the consequences of PLA_2 action in certain chronic inflammatory conditions, such as rheumatoid arthritis and asthma. To this end, a clear understanding of the interaction of PLA_2 with substrates is required.

On the other hand, PLA_2 is probably one of the best studied enzymes catalyzing a chemical reaction at the lipid–water interface (Volwerk & de Haas, 1981; Dennis, 1983; Jain & Berg, 1989). For most lipolytic enzymes, including PLA_2, the hydrolytic activity rate on aggregated forms of the substrate (micelles, mixed micelles, monolayers, and bilayers) is much higher than the activity on soluble substrates that are monomolecularly dispersed in solution. This phenomenon is known as "interfacial activation" and is not yet completely understood even though several models have been suggested in order to account for it (Barlow et al., 1988): (1) an "interfacial recognition site" model, according to which a conformational change takes place in the enzyme at the interface; (2) a "dual phospholipid" model in which an activator phospholipid accelerates the rate of hydrolysis of another phospholipid upon binding to a specific activator site; and (3) a "substrate effect" model in which the restrictions induced in the substrate upon packing lead to a productive encounter with the active center.

PLA_2s are found both intracellularly and extracellularly. Among the extracellular PLA_2s, the best known families are the pancreatic and cobra venom enzymes which are both type I PLA_2s, of which the best characterized ones appear to act in monomeric form (Scott et al., 1990). Yet two major differences make them distinct: (i) in structural terms, part of the surface loop comprising positions 57–70 is deleted in cobra venom PLA_2s (Davidson & Dennis, 1990); (ii) in kinetic terms, pancreatic PLA_2s are activated by negatively charged substrates whereas cobra venom PLA_2s are activated by substrates containing phosphocholine (Kuipers et al., 1989a; Yuan et al., 1990; Noel et al., 1990). By means of protein engineering and X-ray crystallographic techniques (Kuipers et al., 1989a), it has been shown that removal of residues 62–66 from the surface loop 57–70 of porcine pancreas PLA_2 increases the catalytic activity rate on choline derivatives and decreases this rate on negatively charged substrates. In the present work we advance a structural explanation to account for this fact based on a model according to which cobra venom PLA_2s, in addition to the active site, do have another binding site for the choline head of choline derivatives on this surface loop, thus lending further support to the dual phospholipid model.

Materials and Methods

Force Field and General Modeling Parameters. In our calculations we followed a molecular mechanics approach to build up the molecular models and refine their energy, making use of the AMBER suite of programs (Seibel et al., 1989) and considering all the atoms explicitly. The necessary parameters for both the enzymes and the solvent were taken from the AMBER database. The atoms of phospholipid molecules and derivatives were assigned the van der Waals and hydrogen-

[†] This research has been financed in part by Laboratorios Menarini S.A., Badalona, Spain, Comisión Interministerial de Ciencia y Tecnología (CICYT), and the University of Alcalá de Henares, Madrid, Spain.

* Author to whom correspondence should be addressed.

0006-2960/92/0431-2887$03.00/0

bonding parameters of corresponding AMBER atom types; the additional parameters necessary were obtained in accordance with a well-established interpolation method (Weiner et al., 1984), and point charges were calculated so as to reproduce the molecular electrostatic potential (MEP) (Ferenczy et al., 1990). The electrostatic potential was calculated 1.4 Å along the surface normal vector from a given molecular surface point and represented at the surface point itself. The molecular surfaces displayed in Figure 3 were calculated by using the molecular surface program of Connolly (1981), the dots being color-coded according to the MEP value on that point. The interactive graphics program INSIGHT (1991) was used throughout. All of the programs were implemented on a CYBER 910B-537 workstation.

Molecular Modeling of the Enzyme. We have modeled the three-dimensional structure of PLA_2 from the *Naja naja kaouthia* (cobra) venom CMIII fraction (NNK-PLA_2), on the basis of crystallographically determined porcine pancreatic PLA_2 with segment 62–66 deleted (Δ62–66 pp-PLA_2) (Kuipers et al., 1989a) and bovine pancreatic PLA_2 (bp-PLA_2) (Dijkstra et al., 1981), available from the Protein Data Bank (Bernstein et al., 1977; entries 3p2p and 1bp2, respectively). The choice of this enzyme for our study rather than the one from *Naja naja naja* venom often used in biochemical experiments is due to the fact that whereas both enzymes possess an identical surface loop and display a very similar kinetic behavior (Yuan et al., 1990), NNK-PLA_2 offers some advantages from a modeling perspective: (i) the modeling process is facilitated by the lower number of degrees of freedom in the amino acids found in homologous positions, and (ii) interferences in the interaction between phosphocholine and loop 57–70 are prevented to a larger extent due to the lower number of formal charges in NNK-PLA_2. The structure was modeled by superimposing the known structures of bp-PLA_2 and Δ62–66 pp-PLA_2 according to the criterion of Renetseder et al. (1985). This same criterion was used to align the sequences and to define the conserved regions in the starting structures (Greer, 1990). The NNK-PLA_2 sequence was then aligned (Figure 1), making use of the HOMOLOGY module in the INSIGHT suite of programs (1991) and standard procedures (George et al., 1990). The atomic coordinates of the conserved regions in bp-PLA_2 and Δ62–66 pp-PLA_2 were divided into the necessary number of segments so as to minimize the number of mutations required to construct the NNK-PLA_2 molecule. We included the crystallization water molecules from subunit A of Δ62–66 pp-PLA_2 in order to consider those water molecules important for maintaining the structure. Where mutations were required, these were performed, endeavoring to make the environment of the mutated residue that of the new protein, and maximizing the number of atoms in the new residue that superimposed on the "old" one in those amino acids of similar size and electrostatic character, because these tend to retain the same conformation in similar proteins (Schiffer et al., 1990). For residues having more degrees of freedom than the original amino acid, the LECS (lowest energy conformational search) method was used (Schiffer et al., 1990) to select the conformation of the new residue. In brief, the starting conformations of the "new" residue were selected by using a library of conformers (Ponder & Richards, 1987), choosing those which maintained the χ_1 angle with respect to the old residue. For each of the conformers chosen, an energy minimization process was performed in the following way: A bath of equilibrated TIP3P water molecules, generated by means of a Monte Carlo simulation (Jorgensen et al., 1983), was centered on the atomic coordinates of the Cα of each residue, and those water molecules found less than 2.4 Å from any atom were eliminated, as well as those further away than 12 Å from the Cα atom. Initially, only the water molecules were minimized in order to relax the sphere of water without disrupting the enzyme; then, the whole structure within 11 Å of the sphere was minimized, keeping the remainder of the structure fixed in its original position. Each minimization was carried out until the gradient converged to an rms of 0.1 kcal mol^{-1} $Å^{-1}$. If a given conformer did not converge after 1000 cycles, the minimization was deemed complete. Since water was incorporated explicitly, it was not possible to compare the relative energies obtained for the different conformers since the number of water molecules necessary to solvate the residue can be different depending on its conformation. For this reason, their solvation free energies (SFE) were computed according to the method of Eisenberg and McLachlan (1986). The conformer selected was that presenting the lowest SFE. No universally accepted criterion does really exist to correctly model the substitutions in the side chains of homologous proteins when the new residue is endowed with a greater number of degrees of freedom and is exposed to the solvent (Schiffer et al., 1990). We have selected the SFE as a criterion since the conformation of the external residues in proteins appears to be that showing the lowest SFE (Schiffer et al., 1990). One of the problems in using this method is that very similar SFE values can be calculated for different conformers. Yet this can reflect the accessibility of the amino acid to different conformational states in solution. Therefore, computation of the SFE values seems to us the least unsatisfactory of the possible options. The whole model was then subjected to an energy minimization process in order to obtain the final structure using a distance-dependent dielectric constant and a nonbonded cutoff of 9.5 Å. First, the steepest descent minimization algorithm was used until the gradient converged to an rms of 0.1 kcal mol^{-1} $Å^{-1}$, incorporating into the force field a harmonic force constant (5 kcal mol^{-1} $Å^{-1}$) to keep the geometries of the catalytic network and the calcium binding loop in agreement with those found in bp-PLA_2 (Dijkstra et al., 1981). Then, the energy of the entire system was refined using the conjugate gradient method until convergence, as judged by the same criterion as before.

Evaluation of the Model. In addition to calculating the root-mean-square (rms) displacement of the Cα atoms, the following three currently utilized criteria were used to evaluate the quality of our model-built structure:

(*1*) *Empirical Free Energy Function.* The method of Eisenberg and McLachlan (1986) was employed to compute the SFE of our model and that of each starting structure by using the atomic coordinates. A theoretical value of SFE was also calculated as a function of the number of amino acids (N) in each protein according to the relation: SFE = $15.3-1.13(N)$ (Chiche et al., 1990). It has been proposed that the deviation of the theoretical estimate from the value calculated from the atomic coordinates can be used as an index of model correctness (Chiche et al., 1990).

(*2*) *Surface Accessibility.* The surface accessibility (SA) of all non-hydrogen atoms was calculated by using the method of Lee and Richards (1971). A 1.4-Å probe was used for these computations. The accessible surface area of a globular monomeric protein was calculated from the molecular weight by using the following relationship (Chotia, 1975): SA = $11.12M_w^{2/3}$. The SA index is defined as the ratio of the SA calculated by using the atomic coordinates of the model to the average SA of a globular protein and should approximate 1.0 for a correctly folded protein.

(3) Molecular Mechanics Potential Energy Function. The potential energies of the model protein and both starting structures were computed using the AMBER force field. For this calculation the X-ray structures were subjected to 300 steps of steepest descent energy minimization using an 8-Å cutoff and a distance-dependent dielectric function. Whereas it is true that potential energy functions cannot discriminate between correct and incorrect models, it is also true that the potential energy of a correct model must be low (Novotny et al., 1984).

Molecular Modeling of the Phospholipid Analogues. Coordinates for choline *n*-heptyl phosphate (C7PC) were derived from the crystal structure of 2,3-dimyristoyl-D-glycero-1-phosphocholine (Pearson & Pascher, 1979) and subsequent model building in INSIGHT. The geometry was fully optimized using the semiempirical molecular orbital method MNDO within the AMPAC program (Dewar & Stewart, 1986). Ethanolamine *n*-heptyl phosphate (C7PE) and dioctanoylphosphatidylcholine (diC8PC) were modeled from C7PC using the same methodology.

Model Building and Energy Minimization of the Complexes. Docking of C7PC into the phosphocholine binding site was achieved by means of the DOCKING module within INSIGHT. The energy of the entire system was minimized in AMBER until the gradient converged to an rms of 0.1 kcal mol^{-1} $Å^{-1}$. Previous superimposition of the three different enzymes (NNK-PLA_2, Δ62–66 pp-PLA_2, and bp-PLA_2) highlighted the corresponding binding sites in the other two enzymes and facilitated docking of C7PC into the respective regions. Minimization of the other two complexes was carried out under the same conditions, and the interaction energies were calculated by using the ANAL module in AMBER. No major conformational changes were observed in NNK-PLA_2 nor were any unfavorable contacts detected. Docking of C7PE in the activator site of NNK-PLA_2 was accomplished by substituting its coordinates for those of C7PC in the complex and endeavoring to make as many favorable contacts as possible.

Docking of diC8PC into the active site of NNK-PLA_2 was accomplished by taking into consideration the distances provided by Thunnissen et al. (1990) for the interactions of (*R*)-2-(dodecanoylamino)-1-hexanol phosphoglycol.

Similarity Calculations. The ASP (automated similarity package) program (Burt et al., 1990) was employed to evaluate similarity indices (SI). Such calculations provide a useful approach to theoretical drug design and were here applied to part of the enzymes. The charge distribution of two superimposed molecules, a and b, may be compared using an index (H_{ab}) defined as (Hodgkin & Richards, 1987)

$$H_{ab} = \frac{2\int \rho_a \rho_b \, dV}{\int \rho_a^2 \, dV + \int \rho_b^2 \, dV} \quad (1)$$

where ρ_a and ρ_b are the electron densities of molecules a and b, respectively. The numerator is a measure of the charge density for two superimposed molecules, and the denominator is a normalization factor so that the function takes a range of values from 0 to 1, where 1 indicates identical electron densities. Such an equation has been primarily used to compare MEPs in small molecules (Burt et al., 1990). Calculated indices range from +1.0 (perfect similarity) to −1.0. These parameters are proven discriminators of biological activity. A grid is calculated, and the electrostatic potential (V) at each grid point ($\mathbf{r}$) is computed according to the equation

$$V(\mathbf{r}) = \sum_{i=1}^{i=n} \frac{q_i}{|\mathbf{r} - \mathbf{r}_i|} \quad (2)$$

Table I: rms Displacements of Cα Atoms between the Reference Structures and the Modeled Enzyme

	bp-PLA_2	bp-PLA_2[a]	Δ62–66 pp-PLA_2	NNK-PLA_2
bp-PLA_2	0			
bp-PLA_2	0	0		
Δ62–66 pp-PLA_2	1.12	0.90	0	
NNK-PLA_2	1.55	1.31	1.19	0

[a] bp-PLA_2 excluding the loop comprising residues 57–70/60–72.

Table II: Parameters for Evaluation of Our Modeled Structure in Comparison with the Two Reference Crystal Structures

protein	no. of amino acids	E_{pot}[a]	SA index[b]	SFE(c)	SFE(t)	% dev[c]
bp-PLA_2	123	−2078	1.07	−180	−124	−45
Δ62–66 pp-PLA_2	120	−1747	1.07	−178	−120	−48
NNK-PLA_2	119	−2149	1.01	−174	−119	−46

[a] Potential energy (E_{pot}) and solvation free energies (SFE), derived both from the atomic coordinates (c) and from the number of amino acids (t), are expressed in kcal/mol. [b] Surface accessibility index. [c] % dev = [(SFE(t) − SFE(c))/SFE(t)] × 100. See text for more details.

where q_i is the point charge on the atom i, as taken from the AMBER database, $\mathbf{r}_i$ is the position of atom i, and n is the number of charges in the molecule.

Results and Discussion

Molecular Modeling of NNK-PLA_2. NNK-PLA_2 was modeled as a monomeric enzyme since it does not present the residues necessary for formation of a functional dimer (Renetseder et al., 1985). In dimeric PLA_2s dimer stabilization arises both from the hydrogen bond between Glu-6 in one subunit and Trp-31 and His-34 in the other one and from the electrostatic interaction between Asp-49 in the former and Lys-69 in the latter. In NNK-PLA_2 this is not possible due to the replacement of Glu-6 with Lys, Trp-31 with Arg, His-34 with Ser, and Lys-69 with Tyr. Recent crystallographic results (White et al., 1990) on *Naja naja atra* venom PLA_2 support this assumption.

The overall structure of the NNK-PLA_2 model is similar to that of the starting proteins and conserves the same secondary structure elements. Table I gives a comparison of rms displacements of Cα atoms in these molecules. The rms between NNK-PLA_2 and bp-PLA_2 is 1.55 Å whereas the reported rms between the crystal structure of NNA-PLA_2 and bp-PLA_2 is 0.99 Å (White et al., 1990). The largest displacements between NNK-PLA_2 and bp-PLA_2 are observed in the C-terminus and in loop 57–70, which in the model is similar to that found in the mutant porcine enzyme. The correctness of our model structure was assessed by means of different criteria (cf. Materials and Methods), providing values in the same range as those found for crystal structures (Table II), which indicates that our model molecule is a reasonable approximation to the structure of NNK-PLA_2.

It should be noticed that the active site is highly conserved in the enzymes studied, despite marked differences in their catalytic activity (Kuipers et al., 1989a). As pointed out by crystallographic studies of PLA_2 with a substrate-derived inhibitor (Thunnissen et al., 1990) and a phosphonate transition-state analogue (White et al., 1990), the active site is not able to discriminate among the different phospholipids since binding of the phospholipid takes place with its polar head oriented toward the solvent so that no direct specific interactions occur with the enzyme.

When NNK-PLA_2 and pancreatic PLA_2s are compared (Figure 1), it is observed that, similarly to what is the case

```
               10        20        30        40        50        60
          *=*==***==*=*=********==*=======*===================*=====*===*==**

bp      1 ALWQFNGMIKCKIPSSEPLLDFNNYGCYCGLGGSGTPVDDLDRCCQTHDNCYKQAKKLDS 60
pp      1 ALWQFRSMIKCAIPGSHPLMDFNNYGCYCGLGGSGTPVDELDRCCETHDNCYRDAKNLDS 60
hp      1 AVWQFRKMIKCVIPGSDPFLEYNNYGCYCGLGGSGTPVDELKRCCQTHDNCYDQAKKLDS 60
Δpp     1 ALWQFRSMIKCAIPGSHPLMDFNNYGCYCGLGGSGTPVDELDRCCETHDNCYRDAKNLSG 60
NNN     1 NLYQFKNMIKCTVPSR.SWWDFADYGCYCGRGGSGTPVDDLDRCCQVHDNCYNEAEKISG 59
NNA     1 NLYQFKNMIQCTVPSR.SWWDFADYGCYCGRGGSGTPVDDLDRCCQVHDNCYNEAEKISG 59
NNK     1 NLYQFKNMIQCTVPSR.SWWNFADYGCYCGRGGSGTPVDDLDRCCQVHDNCYDEAEKISG 59
          aaaaaaaaaaaa------aaaa------------------aaaaaaaaaaaaaaaaaaa--

               70        80        90       100       110       120
          =******==*====*===**===****===*=*======*=====*=====*=***===*=**=*=

bp     61 CKVLVDNPYTNNYSYSCSNNEITCSSENNACEAFICNCDRNAAICFSKVPYNKEHKNLD.KKNC..  123
pp     61 CKVLFDNPYTESYSYSCSNTEITCNSKNNACEAFICNCDRNAAICFSKAPYNKEHKNLDTKKYC..  124
hp     61 CKFLLDNPYTHTYSYSCSGSAITCSSKNKECEAFICNCDRNAAICFSKAPYNKAHKNLDTKKYCQS  126
Δpp    61 C.....YPYTESYSYSCSNTEITCNSKNNACEAFICNCDRNAAICFSKAPYNKEHKNLDTKKYC..  119
NNN    60 C.....WPYFKTYSYECSQGTLTCKGDNNACAASVCDCDRLAAICFAGAPYNDNNYNIDLKARCQ.  119
NNA    60 C.....WPYFKTYSYECSQGTLTCKGGNNACAAAVCDCDRLAAICFAGAPYNDNDYNINLKARCQE  120
NNK    60 C.....WPYFKTYSYECSQGTLTCKGGNNACAAAVCDCDRLAAICFAGAPYNNNNYNIDLKARCQ.  119
          -aaaaa-------ββββββββββββ-----aaaaaaaaaaaaaaaaaaaaa-----------------
```

FIGURE 1: Alignment of sequences of several type I PLA_2s from different sources: bp, bovine pancreas; pp, porcine pancreas; hp, human pancreas; Δpp, Δ62–66 porcine pancreas; NNN, *N. naja naja*; NNA, *N. naja atra*; NNK, *N. naja kaouthia*. The upper symbol = means that the amino acid in the corresponding position belongs to the same group and is conserved in both families, whereas the * stands for an amino acid that is conserved within each family. N,Q, S,T, D,E, and L,I,V are amino acids considered to belong to the same group, respectively. A specific amino acid is considered conserved within each family if at least two members of the family have it in that position. The lower symbols represent secondary structure elements: α-helices (α), antiparallel β-sheets (β), and loops, turns, or coils (–). The upper sequence numbering scheme refers to the relative *3-D position* of the amino acid, taking bp-PLA_2 as a reference, whereas the lateral figures refer to *primary sequence* numbering. Residues making up the putative activator site in cobra venom PLA_2s are shown in bold face.

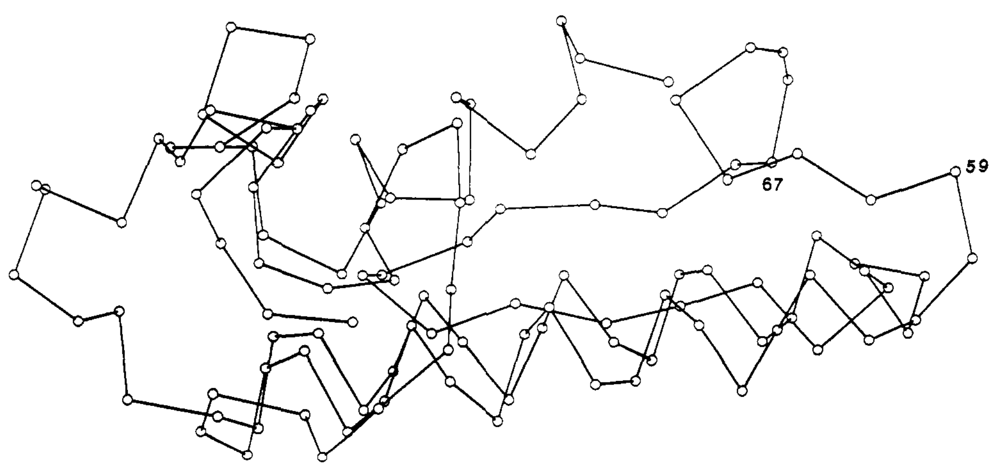

FIGURE 2: Boat shape of NNK-PLA_2 (only α carbon atoms are displayed). The residues making up the active site and the calcium binding loop are essentially in the same positions as in pancreatic PLA_2s. In this view the IRS (see text) is located in the upper part of the molecule. Primary sequence residues 59 and 67 have been labeled (see Figure 1 legend for details).

in other protein families, mutations and deletions take place mainly in surface loops. This fact is particularly important in PLA_2s, due to their characteristic "boat" shape (Figure 2), the "hull" being formed by definite elements of secondary structure (excluding helices A and B) and the "deck" being made up of the loops connecting these elements together at the same face of the molecule (along with helices A and B). This face is called interfacial recognition surface (IRS) and surrounds the entrance to the active site. It is precisely this face which has been related to the interaction with phospholipid aggregates, so that it is very likely that PLA_2s use this molecular evolutionary mechanism to achieve the required selectivity toward their respective physiological substrates. Comparison also shows the similarity regarding the peptide backbone *except for* the above-mentioned surface loop; the similarity in this loop region, however, is *also* high for Δ62–66 pp-PLA_2. Because the rest of the structure is nearly identical for pp-PLA_2 and Δ62–66 pp-PLA_2, and since Δ62–66 pp-

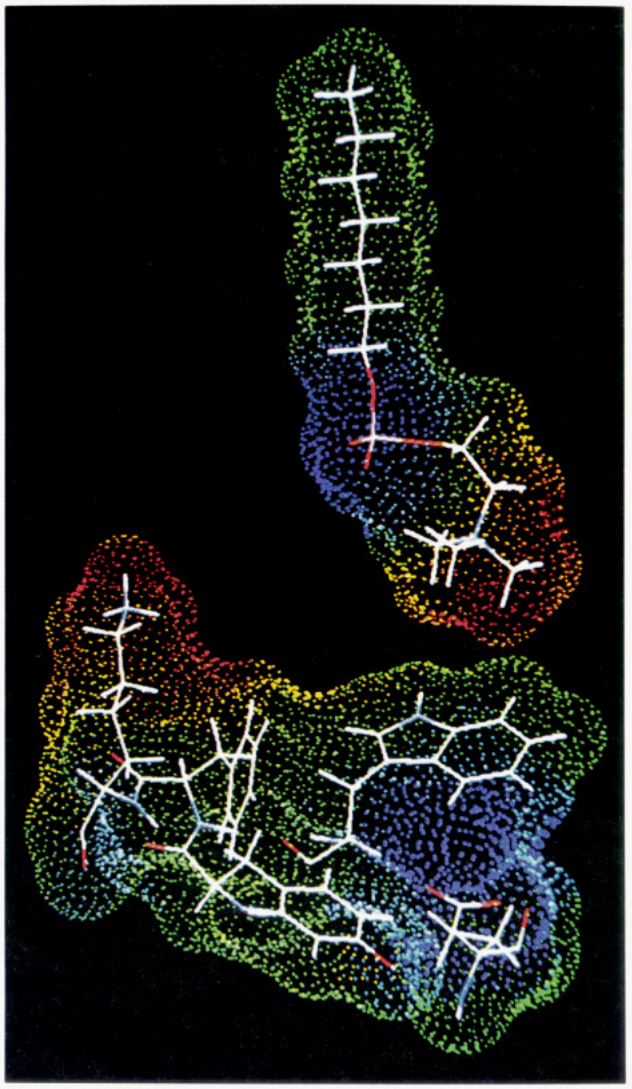

FIGURE 3: Steric and electrostatic complementarity between the putative activator site in the NNK-PLA_2 enzyme (MEP ranging from −33.4 to 35.3 kcal/mol) and the C7PC choline head (MEP ranging from −22.4 to 17.6 kcal/mol) prior to docking. The picture shows the MEP displayed on the van der Waals surface of each molecule and color-coded so that the most positive regions are in red and the most negative ones in blue with intermediate values ramping smoothly.

PLA_2 displays an increased catalytic activity on dioctylphosphatidylcholine *and* a decreased activity toward negatively charged substrates with respect to native pp-PLA_2 (Kuipers et al., 1989a), it seems reasonable to assume that the most important structural basis of specificity toward separate phospholipids on the part of pancreatic and cobra venom PLA_2s lies in that loop.

Table III: Correlation between Calculated Enthalpies for C7PC Binding to the Putative Activator Site, Catalytic Activities on Dihexanoylphosphatidylcholine Micelles, and Similarity Indices for Different PLA_2s

	BE[a]	$k_{cat}/10^b$	SI[c]
cobra venom PLA_2	−71.2	83.0	77.0
Δ62–66 pp-PLA_2	−7.3	8.0	18.2
pancreatic PLA_2	−0.4	0.5	25.0

[a] Binding enthalpy (kcal/mol) of C7PC to the putative activator site. [b] Catalytic activity rate (s^{-1}) on dihexanoylphosphatidylcholine micelles [see Kuipers et al. (1989a)]. [c] Percentage similarity index between the activator site in each of the enzymes and the phosphocholine binding site in McPC603 (see text).

Indeed, our modeling suggests that in the region of loop 57–70 of NNK-PLA_2 there exists a specific recognition site for phosphocholine derivatives, made up of residues Glu-55, Trp-61, Tyr-63, Phe-64, and Lys-65 exposed toward the IRS. The aromatic residues can recognize the positive charge on the choline head through stabilizing interactions via their electron-rich π systems (cation–π interaction), making up a wall analogous to the first "solvation shell"; long-range electrostatic interactions with Glu-55 would produce a second "solvation shell", and Lys-65 itself would fixate the negative charge of the phosphate (Figure 3). A similar pattern has been recently proposed as a new model of biological binding sites for choline and its derivatives (Dougherty & Stauffer, 1990). In this regard, it is remarkable that the Fab portion of phosphocholine binding immunoglobulin McPC603 (Segal et al., 1974) exhibits a binding site (made up of residues Asp97L, Trp107H, Tyr100L, Tyr33H, and Arg52H) nearly identical with the one we now propose in NNK-PLA_2 for choline derivatives. Furthermore, superimposition of both binding sites shows a striking structural similarity between them (Figure 4). The MEP magnitude and shape are also very similar in both sites as quantitatively expressed by a similarity index close to 80% (Table III). Given the importance of this property in biological recognition, this high index reflects a similar behavior in their molecular interactions and therefore an ability to recognize choline derivatives on the part of NNK-PLA_2. Moreover, a significant structural and electrostatic complementarity is found between our proposed activator site and an *n*-alkylphosphocholine molecule (Figure 3).

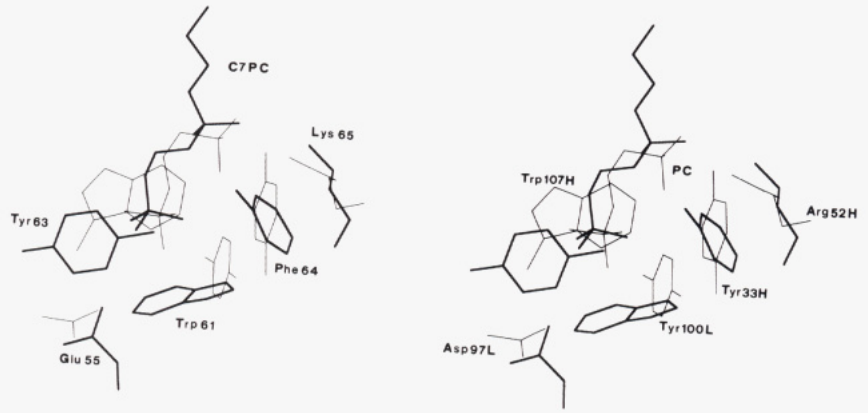

FIGURE 4: Stereoview of the putative activator site (heavy lines) for cobra venom PLA_2s as seen in the modeled NNK-PLA_2–C7PC complex (residue names on the left). Part of the choline *n*-heptyl phosphate (C7PC) molecule is displayed showing the cation–π interaction with the aromatic residues and the electrostatic interaction with Lys-65 and Glu-55. Superimposed on it is the phosphocholine (PC) binding site (thin lines) of McPC603 immunoglobulin (Segal et al., 1974) (residue names on the right).

Table IV: Contributions to the Binding Enthalpy (kcal/mol) According to Equation 3 in the Complexes of C7PC with Different PLA_2s

	ΔE_{PLA_2}	ΔE_{C7PC}		E_{PLA_2-C7PC}			
		MM[a]	MNDO[b]	AS[c]	RE[d]	VW_{SA}[e]	$ELE/HBOND_{SA}$[f]
cobra venom PLA_2	10.0	7.2	5.8	−77.7	−10.7	−6.4	−71.3
Δ62–66 pp-PLA_2	9.0	1.6	4.7	−6.0	−11.9	−4.8	−1.2
pancreatic PLA_2	10.9	2.1	1.7	−0.5	−12.9	−5.0	4.5

[a] C7PC distortion energy calculated by means of molecular mechanics. [b] C7PC distortion energy calculated by means of the MNDO molecular orbital method. [c] C7PC interaction energy with the activator site. [d] C7PC interaction energy with the rest of the enzyme. [e] van der Waals energy contribution to C7PC binding to the activator site. [f] Electrostatic contribution (including the hydrogen-bonding term) to C7PC binding to the activator site.

Interaction between Different PLA_2s and C7PC Monomers. Our model appears to support the dual phospholipid model (Hendrickson & Dennis, 1984): monomeric phosphocholine derivatives activate the enzyme through direct interaction with it, the minimum requirements for a molecule to behave as an activator being an alkyl tail bonded to a phosphocholine head (Plückthun & Dennis, 1982). Besides, pp-PLA_2 Tyr-69 seems to interact with monomeric choline *n*-alkyl phosphate (Kuipers et al., 1990). Therefore, we decided to study the interaction of choline *n*-heptyl phosphate (C7PC) with the putative activator site in bp-PLA_2, Δ62–66 pp-PLA_2, and NNK-PLA_2 in an attempt to find out whether structural changes in these complexes could be related to the catalytic activity of these enzymes on aggregated substrates, in a way consistent with an activation process. bp-PLA_2 was chosen in place of pp-PLA_2 due to the higher resolution of its crystal structure. However, the degree of homology existing between these two enzymes is high, and their kinetic behavior is very similar. On the other hand, although the structure of pp-PLA_2 (Dijkstra et al., 1983) has been determined at a lower resolution than that of bp-PLA_2 (Dijkstra et al., 1981), both of them are very similar except in loop 57–70. This difference appears to be due to contacts in the crystal since protein engineering experiments (van Den Bergh et al., 1989) and NMR data (Fisher et al., 1989) suggest that the porcine loop in solution can adopt the conformation seen in the crystals of the bovine enzyme. Because the putative choline derivatives' recognition region is found on that loop and the experimental studies have been carried out in solution, it seemed more adequate to us to select the bovine enzyme for our calculations.

Predicted binding enthalpies (BE) are shown in Table III and were obtained making use of the simple equation

$$BE = E_{PLA_2-C7PC} + \Delta E_{PLA_2} + \Delta E_{C7PC} \quad (3)$$

where E_{PLA_2-C7PC} is the interaction energy between the enzyme and the phospholipid analogue, ΔE_{PLA_2} is the conformational energy difference for the enzyme upon interaction with the analogue, and ΔE_{C7PC} is the distortion energy of the ligand calculated with respect to the optimized energy of the free molecule. ΔE_{C7PC} was calculated both by molecular mechanics and by the MNDO molecular orbital method and is a measure of the distortion the molecule has to undergo in order to make favorable interactions with the enzymes. The use of the semiempirical method is an additional means of checking that we have calibrated the parameters correctly (Gago et al., 1989).

Two assumptions were made when creating and refining the complexes: (a) in case a conformational change were to take place, this was most likely to occur in loop 57–70 and the first turn of helix A (residues 1–4), since these two regions are the most mobile (Dijkstra et al., 1984) and a conformational change in another region seems unlikely; and (b) interaction between C7PC and its recognition site on the enzyme must occur in a desolvated environment since it emerges from several studies that when the enzyme binds to the interface, this must be desolvated in order for activation to proceed (Jain et al., 1986; Scott et al., 1990).

The respective binding enthalpies are found to parallel the catalytic rate of these enzymes acting on dihexanoylphosphatidylcholine micelles. These data, together with the calculated similarity indices (Table III), point out to the existence of a specific recognition binding site for choline derivatives in cobra venom PLA_2s which is not present in the pancreatic enzymes. Furthermore, upon occupation of this site the enzyme activity toward choline derivatives in aggregated form increases substantially. Even though our sampling has been restricted to only three complexes, we see these differences in interaction energy of about 1 order of magnitude with respect to one another as highly significant, the probability of them being attributed to chance alone seeming very low. This good correlation and the above-mentioned evidence clearly indicate that there exists a recognition site for choline derivatives in cobra venom PLA_2s which (i) is responsible for the selectivity of these enzymes toward their substrates and (ii) behaves as an activator site and is involved in the process of interfacial activation.

Decomposition of the interaction energies into their fundamental contributions (Table IV) shows that this interaction is mainly of an electrostatic nature due to the interactions between the C7PC molecule and both the aromatic ring π systems and the charged groups (note in Figure 3 that the positive charge on C7PC is mainly found on the methyl groups in the choline head). The residues giving rise to the strongest interactions are Glu-55 and Lys-65. This is consistent with the quantitative results obtained for the interaction energies between McPC603 and phosphocholine (Novotny et al., 1989), according to which Arg appears to have a strongly "energetic" role, and also with recent site-directed mutagenesis experiments (Glokshuber et al., 1991) which show that binding of the quaternary ammonium group requires a negative charge at the bottom of the binding pocket in McPC603. In this respect it is interesting to highlight that whereas Glu-55 is conserved in most cobra venom PLA_2s, this same position is occupied by Lys in the pancreatic enzymes (Lys-56) and by a noncharged amino acid in dimeric PLA_2s (this residue is a contact region between the two subunits).

The kinetic behavior of Δ62–66 pp-PLA_2 (Kuipers et al., 1989a) can thus be rationalized: the small increase in activity with respect to native pp-PLA_2 is due to the moderately favorable cation–π interactions involving Tyr-62 and Tyr-64, together with the slightly unfavorable interactions involving the charged residues, whose charge distribution is found inverted in relation to that in NNK-PLA_2 (Figure 5a). These latter interactions appear to be less unfavorable than might be expected (Table V), in the case of lysine, due to the "insulating" effect of the aromatic rings surrounding the choline head and, in the case of glutamic acid, due to its being located sufficiently separated from the phosphate group (Figure 5b). Nevertheless, in bp-PLA_2 the unfavorable interactions between lysine and the choline head are far more

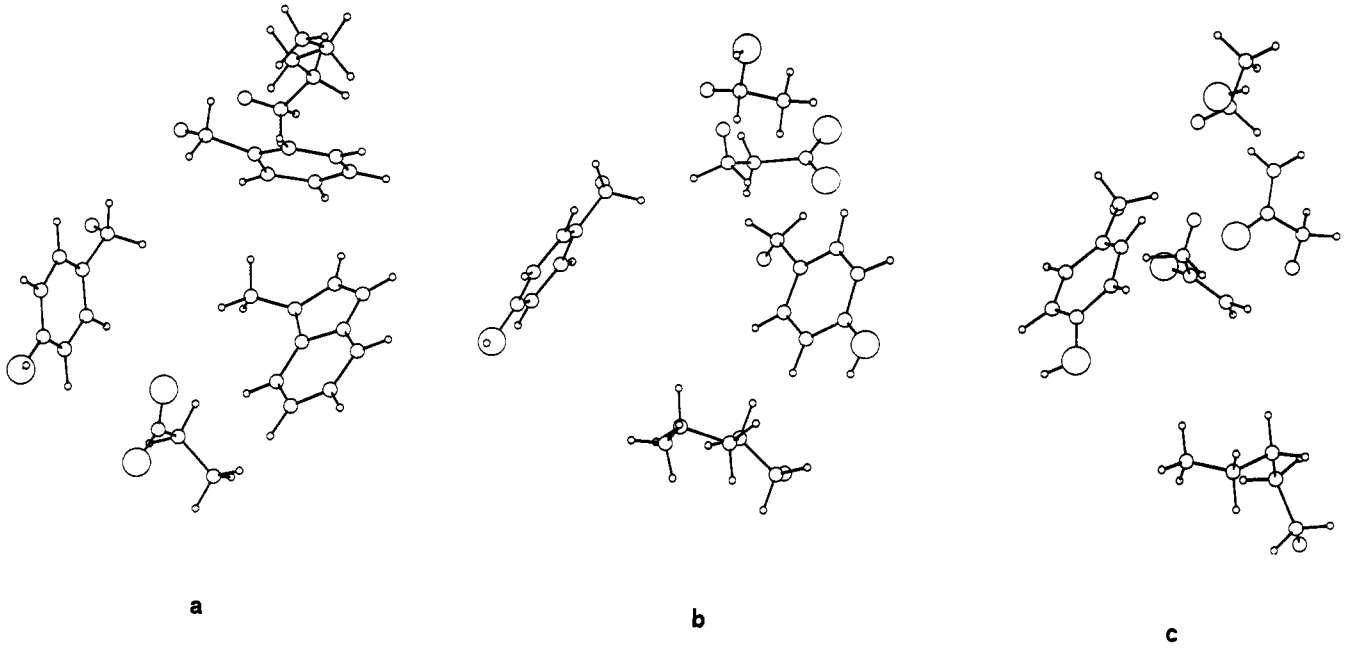

FIGURE 5: Spatial disposition of the residues making up the putative activator site in the different PLA_2s studied. For clarity only the side chains are displayed. (a) NNK-PLA_2; (b) Δ62–66 pp-PLA_2; (c) bp-PLA_2.

Table V: Major Energy Contributions of Individual Residues to the Binding Enthalpy (BE_{PLA_2-C7PC}) of C7PC in the Putative Activator Site

	cobra venom PLA_2		Δ62–66 pp-PLA_2		pancreatic PLA_2	
position[a]	res	$E_{res-C7PC}$	res	$E_{res-C7PC}$	res	$E_{res-C7Pc}$
56	Glu	−25.0	Lys	5.9	Lys	13.8
67	Trp	−3.2	Tyr	−3.7	Asn	−9.0
69	Tyr	−4.5	Tyr	−4.5	Tyr	−4.6
70	Phe	−7.0	Thr	−7.2	Thr	−1.8
71	Lys	−38.0	Glu	3.7	Gln	1.1

[a] Numbering refers to the spatial position of the residue in the enzyme, taking bp-PLA_2 as a reference (cf. Figure 1), according to the criterion of Renetseder et al. (1985).

important (since the lack of a sufficient number of aromatic residues precludes that insulating effect) and make up the largest single contribution to the low interaction energy between bp-PLA_2 and C7PC (Figure 5c). This same reasoning can help to understand the results of Noel et al. (1990), who found that mutation of a single residue (Lys-56 → Met) in bp-PLA_2 considerably increases its catalytic activity toward choline derivatives. The length of a methionine side chain is similar to that of a lysine residue, but its charge density and lipophilicity are much larger, and comparable to those of an aromatic ring. For this reason methionine can give rise to similar cation–π interactions with the choline head; the electron pairs on the sulfur atom can transfer electron density to the choline head, and the methyl group can create a hydrophobic environment. The result is formation of a recognition site for lecithins rather similar to the phosphocholine recognition site in cobra venom PLA_2s (data not shown). If our reported model is correct, replacement of Lys-56 and Asp-66 by Asp and Lys, respectively, in Δ62–66 pp-PLA_2 should provide a suitable "electrostatic environment" for the binding of a phosphocholine head in that region, and the new double mutant should display an activity toward choline derivatives similar to that found in cobra venom PLA_2s.

Interaction between NNK-PLA_2 and C7PE Monomers. An activator site such as this should also show differential binding affinity for choline and ethanolamine derivatives, according to experimental evidence (Plückthun & Dennis, 1982). Our calculations demonstrate that the respective interaction energies between either C7PC or ethanolamine *n*-heptyl phosphate (C7PE) and the activator site in NNK-PLA_2 differ in about 40% (Table VI). This difference indicates that the activator site displays selectivity toward choline derivatives. Since the activator site is the major contributor to the interaction energy (Table VI) and it is just a small portion of the relatively large IRS, enzyme affinity for the micelle should not change substantially. In fact, cobra venom PLA_2s' affinities for phosphatidylcholine or phosphatidylethanolamine mixed micelles do not differ significantly (Hendrickson & Dennis, 1984).

It is interesting to analyze the specific contributions to this difference in interaction energies: we find the largest one being due to Lys-65 (20.6 kcal/mol), followed by Glu-55 and Tyr-63 (around 4.5 kcal/mol each). At first sight, the difference in Lys-65 is surprising since in both cases there exists a phosphate–lysine interaction with similar distances. Nevertheless, the volume of the ethanolamine head is far smaller and its charge density is much larger than those of the choline head. This results in a larger interaction energy between ethanolamine and phosphate compared to that between choline and phosphate; the N–O distance is 2.6 Å in C7PE–NNK PLA_2

Table VI: Breakdown of the Interaction Energy (kcal/mol) of the Ligand (C7PC or C7PE) in the Putative Activator Site of NNK-PLA_2

		ΔE_{ligand}		$E_{PLA_2-ligand}$						
	ΔE_{PLA_2}	MM[a]	MNDO[b]	Glu-55[c]	Trp-61	Tyr-63	Phe-64	Lys-65	RE[d]	BE[e]
C7PC	10.0	7.2	5.8	−25.0	−3.2	−4.5	−7.0	−38.0	−10.7	−71.2
C7PE	3.4	3.3	0.7	−20.9	−1.5	0.4	−5.1	−17.4	−7.3	−45.1

[a] Ligand conformational energy change upon binding (molecular mechanics). [b] Ligand conformational energy change upon binding (MNDO molecular orbital method). [c] Numbering refers to the primary sequence of amino acids. [d] Interaction energy of the ligand with the rest of the enzyme. [e] Total binding enthalpy.

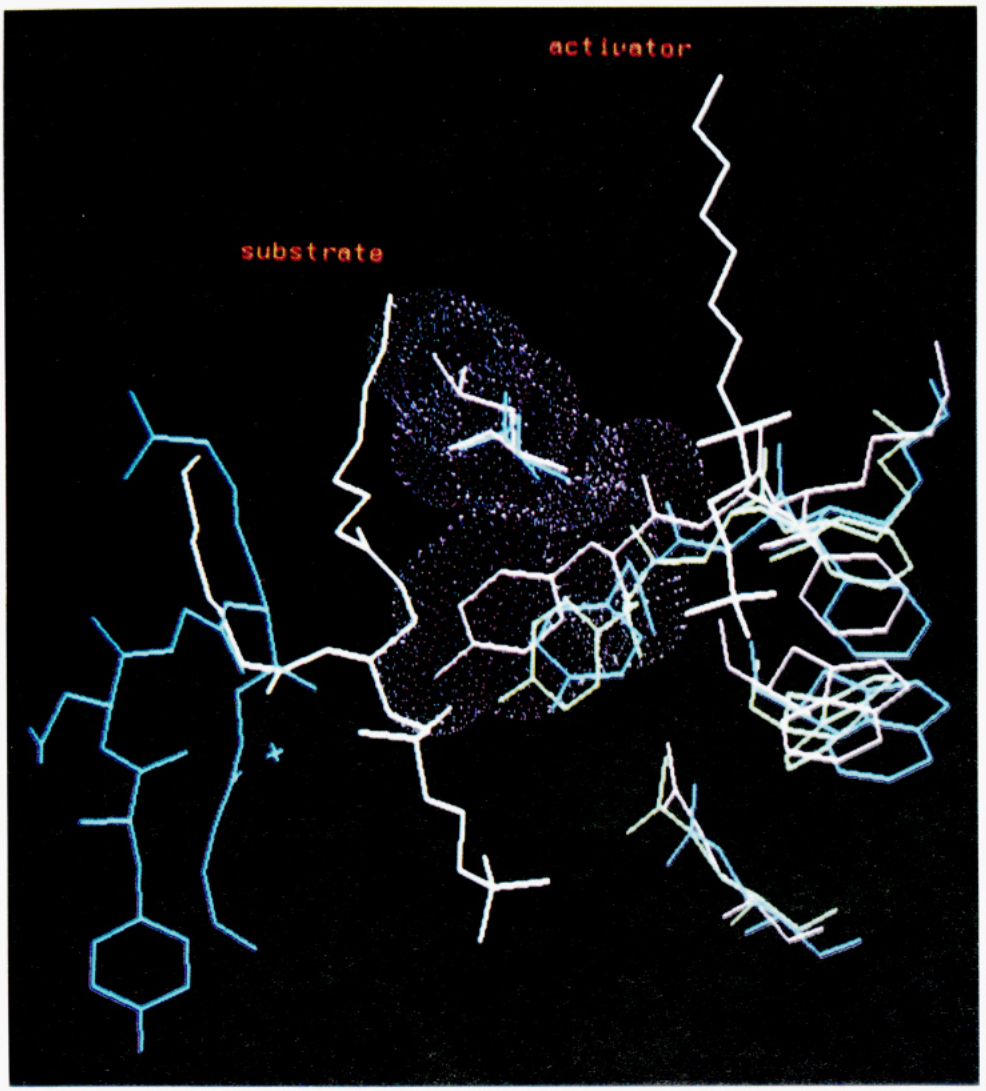

FIGURE 6: Schematic representation of the dual phospholipid model in NNK-PLA_2. The substrate (diC8PC) and the activator (C7PC) phospholipids are shown in white. The model-built NNK-PLA_2 is shown in magenta; the dotted surface highlights the proximity between Leu-2 and Tyr-63 closing the entrance to the active site. The putative activator site of NNK-PLA_2 with docked C7PC is shown in green; note the rotation of the aromatic ring of Tyr-63 thus allowing the entrance of the substrate to the active site. NNK-PLA_2 with substrate bound in the active site is shown in blue.

vs 4.9 Å in C7PC–NNK PLA_2. Consequently, (i) the conformational changes required to fit into the activator site are more difficult to achieve in the case of C7PE, (ii) the ethanolamine–lysine interactions are more unfavorable than those between choline and lysine, and (iii) the screening of the positive charge is less in the C7PE complex. This same reasoning can be applied to the other two residues: the Glu-55 OE2–C7PE N distance is 5.2 Å whereas the distance between Glu-55 OE2 and the nearest methyl group on the choline head is 3.8 Å, hence the stronger electrostatic interactions in the case of C7PC. We observe that the slightly unfavorable interaction between C7PE and Tyr-63 probably arises from the quaternary ammonium group being contacted by the partially positively charged tyrosine aromatic ring edge. It is interesting to note that Tyr-63 has not altered its conformation significantly and continues to close the entrance to the active site, as is the case in the free enzyme. A more detailed discussion on the implications of this effect on the process of interfacial activation is given in the following section.

Implications in the Process of Interfacial Activation. We postulate that in the process of interfacial activation the enzyme binds the micelle through the IRS, a small portion of which—loop 57–70—would be responsible for activation by regulating the degree of solvation and/or the mobility of this region of the interface. Likewise, loss of activity in Ala-1 transaminated bp-PLA_2 (Dijkstra et al., 1984) and bovine pancreas prophospholipase A_2 (Dijkstra et al., 1982) toward aggregated substrates has been put down to increased mobility or disorder in loop 57–70. Note that Tyr-69 is found in this loop, and it plays an important role in monomeric PLA_2s' catalysis because (i) it is involved in recognition of and interaction with aggregated substrates (Kuipers et al., 1989b), (ii) it makes up one of the hydrophobic walls delimiting the active site (Dijkstra et al., 1981), and (iii) it fixates the substrate phosphate group in the active site (Thunnissen et al., 1990). Therefore, the environment of this single residue, in particular its degree of solvation, can have a profound influence on catalysis. According to site-directed mutagenesis experiments, replacement of Tyr-69 with Lys (more flexible and less hydrophobic) in pancreatic PLA_2 reduces the enzymatic activity toward aggregated substrates (Kuipers et al., 1990). It follows from the results of the present work that the putative activator site could contribute to enzyme activation in two ways.

(1) Desolvation of the environment of tyrosine at position 69 (Tyr-63 in NNK-PLA_2): Because of the large volume of

the choline head, its interaction with the activator site demands desolvation of the "activating phospholipid", which would provide the hydrophobic environment at the interface favoring the passage of the "substrate phospholipid" from the membrane to the active site. This view is supported by computational (Dougherty & Stauffer, 1990) and experimental (Shepodd et al., 1986) results indicating that the magnitude of cation–π interactions is quite substantial in an aqueous medium and involves considerable desolvation. On the other hand, it is well-known that quaternary ammonium salts are capable of generating lipophilic ionic pairs with anionic species, a property that is amply utilized in phase-transfer catalysis (Alvarez-Builla et al., 1990).

(2) Opening of the active site: In our NNK-PLA_2 models, binding of choline derivative C7PC to the putative activator site promotes a rotation of ca. 60° in the χ_2 angle of Tyr-63. As a result, this residue opens the entrance to the active site so that penetration of the substrate from the membrane is then possible. In the original model, that is, in the absence of ligand interactions, Tyr-63 occludes this entrance by means of close contacts with Leu-2, thereby preventing direct contact of water with the highly hydrophobic active site (Figure 6).

The preference of cobra venom PLA_2s for choline derivatives over ethanolamine derivatives can be accounted for in terms of the bulkier choline head favoring water exclusion from the activator site. On the other hand, the entrance to the active site is likely to be closed when a ethanolamine derivative binds to the activator site, on the basis of the slightly unfavorable interaction energies we find between C7PE and Tyr-63 and the negligible conformational change observed for this residue.

In our model-built structure no measurable conformational change is observed in the peptide backbone of loop 57–70; nevertheless, the possibility of this change taking place cannot be ruled out completely in the activation mechanism. Likewise, we have characterized the interaction of a monomeric molecule with a putative activator site without taking into consideration other important contributions to the activation mechanism such as the packing of the substrate in the aggregate, the surface area per phospholipid molecule, the surface charge density at the interface, or even the curvature of this interface. It is important to highlight, for instance, that the correlation observed between binding energies and catalytic activity is good when the enzyme acts on dihexanoylphosphatidylcholine micelles but not when acting on C7PC or dioctanoylphosphatidylcholine micelles. We think this difference might be due to the fact that lecithins with alkyl chains less than 14 carbon atoms long form ellipsoidal micelles with a high surface area per phospholipid molecule ($\sim$100 Å^2) whereas those having longer alkyl chains give rise to spherocylindrical micelles with a lower surface area per phospholipid molecule (Lin et al., 1987). Therefore, in the former case the physical effects of the interface are less important and the effects derived from interaction with the activator site predominate. Even so, it is important to point out that pancreatic PLA_2s are more sensitive to surface effects than cobra venom PLA_2s, which seems to be an indication of more recognition specificity on the part of the latter. For example, pancreatic PLA_2s are 100 times more active on dioctanoylphosphatidylcholine than on dihexanoylphosphatidylcholine, whereas activity of cobra venom PLA_2s increases only 4 times. Δ62–66 pp-PLA_2, on the other hand, shows again an intermediate behavior and its activity increases 10 times (Kuipers et al., 1989a).

Differences in loop 57–70 must obey some particular requirement for catalysis in each family of enzymes. A correspondence can be observed between PLA_2 substrate specificity and amino acid sequence in that loop (cf. Figure 1). Whereas in pancreatic PLA_2s an anionic binding site has been proposed involving positions 53, *56*, and 62 (*cationic positions*) along with the NH_2 terminus (Jain et al., 1986), in cobra venom PLA_2s we propose that a pattern of aromatic (positions 67, 69, and 70) and charged (*anionic position 56* and cationic position 71) amino acids specifically recognize choline derivatives. We note that in cobra venom PLA_2s positions 70 and 71 are fixated through hydrogen bonding to the NH_2 terminus, as is the case in pancreatic PLA_2s (data not shown). All of this seems to indicate that both PLA_2 families have modified the same molecular mechanism for their activation, adapting it to their particular requirements. Thus, pancreatic PLA_2s can be activated by negatively charged aggregates such as micelles composed of phospholipids and biliary salts, their physiological substrate. Cobra venom PLA_2s, on the other hand, would have phosphatidylcholine specificity for physiological reasons as well since most of the arachidonic acid is stored in the *sn*-2 position of phosphatidylcholine and phosphatidylethanolamine molecules; therefore, a PLA_2 enzyme rapidly acting on these substrates will be a likely candidate to an agent causing SRS-C production and inflammation (Davidson & Dennis, 1990).

Added in Proof

After this paper was submitted, we were aware of similar choline–protein interactions being reported in a 3-D model of a muscarinic receptor specifically recognizing acetylcholine (Hibert et al., 1991) and suggested by the X-ray structure of acetylcholine esterase (Maelicke, 1991).

Acknowledgments

We thank Dr. David Eisenberg for kindly providing us with his program for calculating solvation free energies, Dr. Chris Reynolds for his program to compute point charges, Oxford Molecular Ltd. for the program ASP, and Biosym Technologies, Inc., for a grant to use their graphics programs.

Registry No. PLA_2, 9001-84-7; C7PC, 79636-16-1; C7PE, 138878-16-7; diC8PC, 41017-85-0; Tyr, 60-18-4; Phe, 63-91-2; Lys, 56-87-1; Glu, 56-86-0; Trp, 73-22-3.

References

Alvarez-Builla, J., Vaquero, J. J., García-Navío, J. L., Cabello, J. F., Sunkel, C., Fau de Casa-Juana, M., Dorrego, F., & Santos, L. (1990) *Tetrahedron 46*, 967–978.

Barlow, P. N., Lister, M. D., Sigler, P. B., & Dennis, E. A. (1988) *J. Biol. Chem. 263*, 12954–12958.

Bernstein, F. C., Koetzle, T. F., Williams, G. J. B., Meyer, E. F., Jr., Brice, M. D., Rodgers, J. R., Kennard, O., Shimanouchi, T., & Tasumi, M. (1977) *J. Mol. Biol. 112*, 535–542.

Burt, C., Huxley, P., & Richards, W. G. (1990) *J. Comput. Chem. 11*, 1139–1146.

Chiche, L., Gregoret, L. M., Cohen, F. E., & Kollman, P. A. (1990) *Proc. Natl. Acad. Sci. U.S.A. 87*, 3240–3243.

Chotia, C. (1975) *Nature 254*, 304–308.

Connolly, M. (1981) *QCPE Bull. 1*, 75.

Davidson, F. F., & Dennis, E. A. (1990) *Biochim. Biophys. Acta 1037*, 7–15.

Dennis, E. A. (1983) *Enzymes (3rd Ed.) 16*, 307–353.

Dewar, M. J. S., & Stewart, J. J. P. (1986) *QCPE Bull. 6*, 24a–24b.

Dijkstra, B. W., Kalk, K. H., Hol, W. G., & Drenth, J. (1981) *J. Mol. Biol. 147*, 97–123.

Dijkstra, B. W., van Nees, G. J. H., Kalk, K. H., Brandenburg, N. P., Hol, W. G. J., & Drenth, J. (1982) *Acta Crystallogr. B38*, 793–799.
Dijkstra, B. W., Renetseder, R., Kalk, K. H., Hol, W. G., & Drenth, J. (1983) *J. Mol. Biol. 168*, 163–179.
Dijkstra, B. W., Kalk, K. H., Drenth, J., de Haas, G. H., Egmond, M. R., & Slotboom, A. J. (1984) *Biochemistry 23*, 2759–2766.
Dougherty, D. A., & Stauffer, D. A. (1990) *Science 250*, 1558–1560.
Eisenberg, D., & McLachlan, A. D. (1986) *Nature 319*, 199–203.
Ferenczy, G. G., Reynolds, C. A., & Richards, W. G. (1990) *J. Comput. Chem. 11*, 159–169.
Fisher, J., Primrose, W. U., Roberts, G. C. K., Dekker, N., Boelens, R., Kaptein, R., & Slotboom, A. J. (1989) *Biochemistry 28*, 5939–5946.
Gago, F., Reynolds, C. A., & Richards, W. G. (1989) *Mol. Pharmacol. 35*, 232–241.
George, D. G., Barker, W. C., & Hunt, L. T. (1990) *Methods Enzymol. 183*, 333–351.
Glokshuber, R., Stadlmüller, J., & Plückthun, A. (1991) *Biochemistry 30*, 3049–3054.
Greer, J. (1990) *Proteins 7*, 317–334.
Hendrickson, H. S., & Dennis, E. A. (1984) *J. Biol. Chem. 259*, 5734–5739.
Hibert, M., Trumpp-Kallmeyer, S., Bruinvels, A., & Hoflack, J. (1991) *Mol. Pharmacol. 40*, 8–15.
Hodgkin, E. E., & Richards, W. G. (1987) *Int. J. Quantum Chem., Quantum Biol. Symp. 14*, 105–110.
Jain, M. K., & Berg, O. (1989) *Biochim. Biophys. Acta 1002*, 127.
Jain, M. K., Maliwal, B. P., de Haas, G. H., & Slotboom, A. J. (1986) *Biochim. Biophys. Acta 860*, 448–461.
Jorgensen, W. L., Chandrasekhar, J., Madura, J. D., Impey, R. W., & Klein, M. L. (1983) *J. Chem. Phys. 79*, 926–935.
Kuipers, O. P., Thunnissen, M. M. G. M., de Geus, P., Dijkstra, B. W., Drenth, J., Verheij, H. M., & de Haas, G. H. (1989a) *Science 244*, 82–85.
Kuipers, O. P., Dijkman, R., Pals, C. E. G. M., Verheij, H. M., & de Haas, G. H. (1989b) *Protein Eng. 2*, 467–471.
Kuipers, O. P., Dekker, N., Verheij, H. M., & de Haas, G. H. (1990) *Biochemistry 29*, 6094–6102.
Lee, B., & Richards, F. M. (1971) *J. Mol. Biol. 55*, 379–400.
Lin, T. L., Chen, S. H., & Roberts, M. F. (1987) *J. Am. Chem. Soc. 109*, 2321–2328.
Maelicke, A. (1991) *Trends Biochem. Sci. 16*, 355–356.
Mobilio, D., & Marshall, L. A. (1989) *Annu. Rep. Med. Chem. 24*, 157–166.
Noel, J. P., Deng, T., Hamilton, K. J., & Tsai, M. D. (1990) *J. Am. Chem. Soc. 112*, 3704–3706.
Novotny, J., Bruccoleri, R. E., & Karplus, M. (1984) *J. Mol. Biol. 177*, 787–818.
Novotny, J., Bruccoleri, R. E., & Saul, F. A. (1989) *Biochemistry 28*, 4735–4749.
Pearson, R., & Pascher, I. (1979) *Nature 281*, 499–501.
Plückthun, A., & Dennis, E. A. (1982) *Biochemistry 21*, 1750–1756.
Ponder, J. W., & Richards, F. M. (1987) *J. Mol. Biol. 193*, 775–791.
Renetseder, R., Brunie, S., Dijkstra, B. W., Drenth, J., & Sigler, P. B. (1985) *J. Biol. Chem. 260*, 11627–11634.
Schiffer, C. A., Caldwell, J. W., Kollman, P. A., & Stroud, R. M. (1990) *Proteins 8*, 30–43.
Scott, D. L., White, S. P., Otwinowski, Z., Yuan, W., Gelb, M. H., & Sigler, P. B. (1990) *Science 250*, 1541–1546.
Segal, D. M., Padlan, E. A., Cohen, G. H., Rudikoff, S., Potter, M., & Davies, D. R. (1974) *Proc. Natl. Acad. Sci. U.S.A. 71*, 4298–4302.
Seibel, G., Singh, U. C., Weiner, S. J., Caldwell, J., & Kollman, P. A. (1989) *AMBER (UCSF): Assisted Model Building with Energy Refinement*, version 3.0, revision A, Department of Pharmaceutical Chemistry, University of California, San Francisco.
Shepodd, M. A., Petti, D. A., & Dougherty, J. (1986) *J. Am. Chem. Soc. 108*, 6085.
Thunnissen, M. M. G. M., AB, E., Kalk, K. H., Drenth, J., Dijkstra, B. W., Kuipers, O. P., Dijkman, R., de Haas, G. H., & Verheij, H. M. (1990) *Nature 347*, 689–691.
van Den Bergh, C. J., Bekkers, A. C. A. P. A., Verheij, H. M., & de Haas, G. H. (1989) *Eur. J. Biochem. 182*, 307–313.
Volwerk, J. J., & de Haas, G. H. (1981) in *Lipid–Protein Interactions*, Vol. 1, p 69, Wiley, New York.
Weiner, S. J., Kollman, P. A., Nguyen, D. T., & Case, D. A. (1986) *J. Comput. Chem. 7*, 230–252.
White, S. P., Scott, D. L., Otwinowski, Z., Gelb, M. H., & Sigler, P. B. (1990) *Science 250*, 1560–1563.
Yuan, W., & Gelb, M. H. (1988) *J. Am. Chem. Soc. 110*, 2666–2667.
Yuan, W., Quinn, D. M., Sigler, P. B., & Gelb, M. H. (1990) *Biochemistry 29*, 6082–6084.